

Electronic Supplementary Material (ESI) for Dalton Trans.

*"Quasi-isotropic SMMs: slow relaxation of the magnetization in polynuclear Cu<sup>II</sup>/Mn<sup>II</sup> complexes"*

**Evangelos Pilichos,<sup>a</sup> Pradip Bhunia,<sup>b</sup> Mercè Font-Bardia,<sup>c</sup> Ashutosh Ghosh,<sup>b,d</sup> Júlia Mayans,<sup>a</sup> Albert Escuer <sup>\*,a</sup>**

<sup>a</sup> Departament de Química Inorgànica i Orgànica, Secció Inorgànica and Institute of Nanoscience (IN<sup>2</sup>UB) and Nanotechnology, Universitat de Barcelona, Martí i Franquès 1-11, Barcelona-08028, Spain.

<sup>b</sup> Department of Chemistry, University College of Science, University of Calcutta, Kolkata 700009, India.

<sup>c</sup> Departament de Mineralogia, Cristal·lografia i Dipòsits Minerals, Universitat de Barcelona, Martí Franquès s/n, 08028 Barcelona (Spain) and Unitat de Difracció de R-X. Centre Científic i Tecnològic de la Universitat de Barcelona (CCiTUB), Solé i Sabarís 1-3. 08028 Barcelona

<sup>d</sup> Rani Rashmoni Green University, Hooghly 712410, West Bengal, India

**1-Instrumental measurements**

**2-Syntheses and characterization.**

**3-Structural aspects.**

**4-Magnetic data.**

## 1-Instrumental measurements

**Physical measurements:** Magnetic susceptibility measurements were carried out on powdered fresh crystals samples with a MPMS5 Quantum Design susceptometer working in the range 30–300 K under magnetic fields of 0.3 T and under a field of 0.03T in the 30 – 2 K range to avoid saturation effects at low temperature. Diamagnetic corrections were estimated from Pascal Tables. Samples for analysis were vacuum dried to remove crystallization solvents. Infrared spectra (4000–400  $\text{cm}^{-1}$ ) were recorded from KBr pellets on a Bruker IFS-125 FT-IR spectrophotometer.

## 2-Syntheses and characterization.

**[Cu<sup>II</sup>L1] metalloligand:** the Cu<sup>II</sup> complex [CuL1] derived from the unsymmetrical di-Schiff base ligand ( $\text{H}_2\text{L} = \text{N}-(\alpha\text{-methylsalicylidene})\text{-N}'\text{-(salicylidene)-2,2-dimethyl-1,3-propanediamine}$ ) was synthesized following the reported method<sup>1</sup> by replacing the 1,3-propanediamine with 2,2-dimethyl-1,3-propanediamine.

**N,N'-Ethylene-bis(3-ethoxysalicylaldimine) (L2)** The Schiff base was synthesized following reported methods<sup>2</sup> mixing an ethanolic solution (15 mL) of ethylenediamine (3 mmols/0.18 g) and o-vanillin (6 mmol/0.91 g). The solution was stirred at room temperature during two hours and the formed yellow solid was collected by filtration and air dried. Yield 80%.

**Synthesis of [(Cu<sup>II</sup>L1)<sub>2</sub>Mn<sup>II</sup>(N<sub>3</sub>)<sub>2</sub>]<sub>2</sub>·2H<sub>2</sub>O (1·2H<sub>2</sub>O).** Mn(ClO<sub>4</sub>)<sub>2</sub>·H<sub>2</sub>O (0.361 g, 1 mmol) was dissolved in a 10 ml of MeOH and to it a 2 ml aqueous solution of NaN<sub>3</sub> (0.130 g, 2 mmol) and a 30 ml methanolic solution of the metalloligand [CuL1] (0.772 g, 2 mmol) were added to it with stirring. After ~ 30 min of stirring, the light green solution was filtered to remove any suspended particles. Brown coloured diffraction quality single crystals were formed within a few days on slow evaporation of solvent. The crystals were collected after 5 days. Yield: 61%. C<sub>40</sub>H<sub>44</sub>Cu<sub>2</sub>MnN<sub>10</sub>O<sub>4</sub>. Calcd: C, 52.74; H, 4.87; N, 15.38. Found C, 52.61; H, 4.99; N, 15.50.

**[{Cu<sup>II</sup>(L2)Mn<sup>II</sup>(H<sub>2</sub>O)<sub>2</sub>(MeOH)}<sub>2</sub>-{Cu<sup>II</sup>(L2)}<sub>2</sub>](ClO<sub>4</sub>)<sub>2</sub>·MeOH (2·MeOH)** To a yellowish methanolic solution (10 ml) of the Schiff base L (0.8 mmol/0.3 g), an aqueous solution (5 ml) of Cu(OAc)<sub>2</sub>·4H<sub>2</sub>O (0.8 mmol/0.159 g) was added. The reaction mixture was placed into a microwaves furnace at 80°C for 30 minutes. The precursor [Cu<sup>II</sup>(L)] was formed as a green precipitate that was filtered and air dried. The freshly formed powder of [Cu<sup>II</sup>(L)] was dissolved in 20 ml of CH<sub>2</sub>Cl<sub>2</sub> and of MeOH (1:1) and Mn(ClO<sub>4</sub>)<sub>2</sub>·6H<sub>2</sub>O (0.25 mmol/0.064 g) was added. The solution was heated in the microwaves furnace for 15 min. at 70°C, resulting a clear dark solution. After 2 days brown crystals, suitable for X-ray diffraction, were formed by layering with diethylether. Yield: 70%. C<sub>55</sub>H<sub>61</sub>Cl<sub>2</sub>Cu<sub>3</sub>MnN<sub>6</sub>O<sub>23</sub>. Calcd: C, 44.32; H, 4.12; N, 5.64. Found C, 44.6; H, 4.4; N, 5.4.

**[( $\mu_{1,1}$ -N<sub>3</sub>)<sub>2</sub>{Cu<sup>II</sup>(L2)Mn<sup>II</sup>}-{Cu<sup>II</sup>(L2)Na<sup>I</sup>(MeOH)(N<sub>3</sub>)<sub>2</sub>}]<sub>2</sub>(ClO<sub>4</sub>)<sub>2</sub> (3)** The complex was prepared following the same procedure than complex 2 but adding NaN<sub>3</sub> (0.4 mmol/0.026 g) to the [Cu<sup>II</sup>(L)] / Mn(ClO<sub>4</sub>)<sub>2</sub>·6H<sub>2</sub>O dissolution. The mixture was introduced to microwaves for 15 min. at 70°C. After two days brown crystals, suitable for X-ray diffraction, were formed by vapor diffusion of diethylether. Yield: 40%. C<sub>74</sub>H<sub>80</sub>Cl<sub>2</sub>Cu<sub>4</sub>Mn<sub>2</sub>N<sub>20</sub>Na<sub>2</sub>O<sub>26</sub>. Calcd: C, 41.41; H, 3.75; N, 13.05. Found C, 41.0; H, 3.7; N, 13.1.

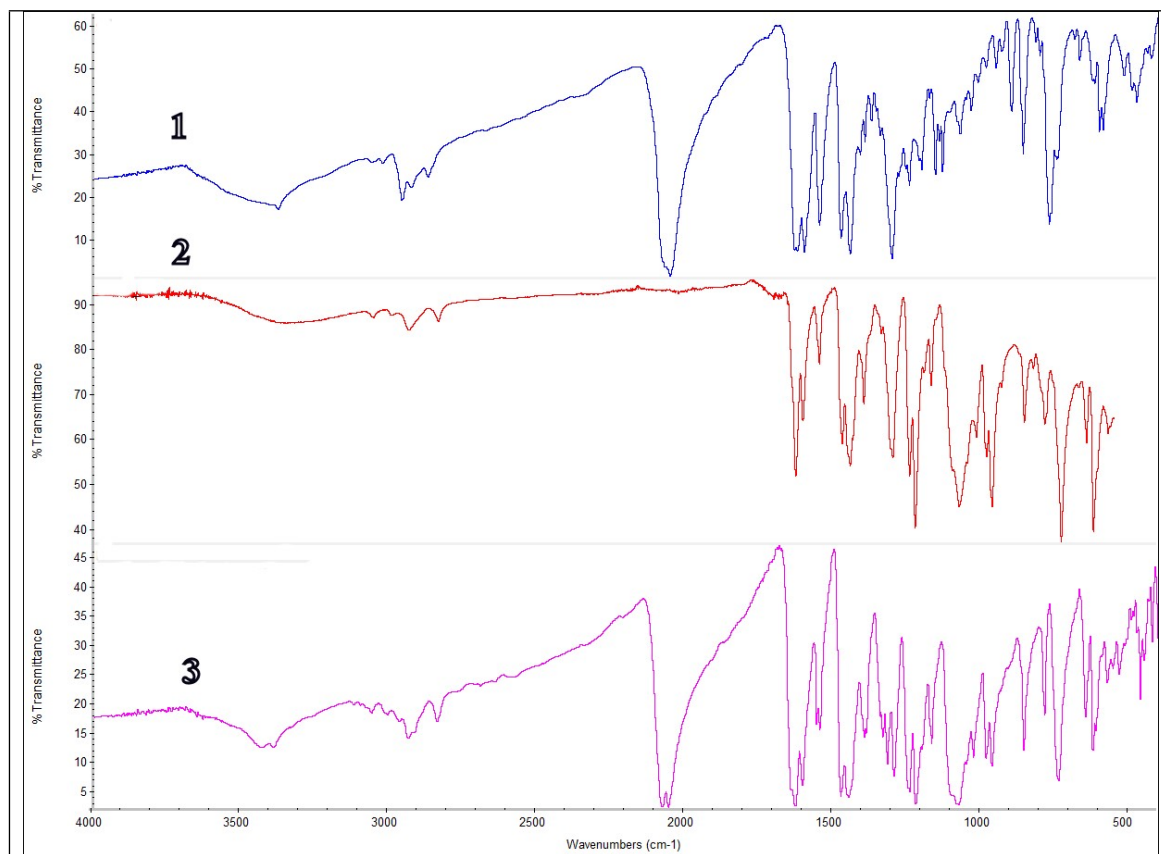


**Figure S1.** IR spectra for complexes **1 - 3**. Characteristic bands: st. C-H 3000-2800 cm<sup>-1</sup>; N=C iminic ~1600 cm<sup>-1</sup>; for **2** and **3**, st. ClO<sub>4</sub><sup>-</sup> 1075 cm<sup>-1</sup>; δ ClO<sub>4</sub><sup>-</sup> 620 cm<sup>-1</sup>. The stretching for the terminal and end-to-end azides for **3** appears differentiated at 2074 and 2055 cm<sup>-1</sup> respectively.

### 3-Structural aspects.

**Table S1.** Crystal data and structure refinement for complexes **1**, **2** and **3**.

	<b>1</b>	<b>2</b>	<b>3</b>
Formula	C <sub>40</sub> H <sub>45</sub> Cu <sub>2</sub> MnN <sub>10</sub> O <sub>5</sub>	C <sub>56</sub> H <sub>66</sub> Cl <sub>2</sub> Cu <sub>3</sub> MnN <sub>6</sub> O <sub>24</sub>	C <sub>74</sub> H <sub>80</sub> Cl <sub>2</sub> Cu <sub>4</sub> Mn <sub>2</sub> N <sub>20</sub> Na <sub>2</sub> O <sub>26</sub>
FW	927.88	1523.60	2146.5
System	Monoclinic	Monoclinic	Triclinic
Space group	C2/c	P21/c	P-1
<i>a</i> /Å	16.839(2)	15.4787(6)	12.3500(6)
<i>b</i> /Å	16.637(2)	22.7556(9)	13.0272(7)
<i>c</i> /Å	16.478(2)	17.7148(7)	13.9308(7)
<i>α</i> /deg.	90	90	107.897(2)
<i>β</i> /deg.	99.467(2)	97.002(1)	91.793(2)
<i>γ</i> /deg.	90	90	94.147(2)
<i>V</i> /Å <sup>3</sup>	4553.3(9)	6193.1(4)	2123.9(2)
<i>Z</i>	4	4	1
<i>T</i> , K	296(2)	100(2)	100(2)
<i>λ</i> (MoK $\alpha$ ), Å	0.71073	0.71073	0.71073
$\rho_{\text{calc}}$ , g·cm <sup>-3</sup>	1.354	1.634	1.678
$\mu$ (MoK $\alpha$ ), mm <sup>-1</sup>	1.250	1.389	1.435
<i>R</i>	0.0609	0.0513	0.0334
$\omega R^2$	0.1774	0.1188	0.0889

**Table S2.** Selected bond distances (Å) and angles (°) for compound **1**.

<b>Bond lengths (Å)</b>			
Cu1 – O11	1.880(3)	Mn(1) – O(11)	2.322(3)
Cu1 – O31	1.893(3)	Mn(1) – O(31)	2.138(3)
Cu1 – N19	1.912(4)	Mn(1) – N(35)	2.163(15)
Cu1 – N23	1.929(5)	Mn(1) – N(35) <sup>#</sup>	2.070(15)
O11 – Cu1 – O31	83.9(1)	O31 – Cu1 – N19	168.3(2)
O11 – Cu1 – N19	94.8(2)	O31 – Cu1 – N23	90.8(2)
O11 – Cu1 – N23	162.7(2)	N19 – Cu1 – N23	93.6(2)
O11 – Mn1 – O31	68.8(1)	O31 – Mn1 – N35	98.3(6)
O11 – Mn1 – N35	83.3(4)	O31 – Mn1 – O31 <sup>#</sup>	142.5(2)
O11 – Mn1 – O11 <sup>#</sup>	81.7(2)	O31 – Mn1 – N35 <sup>a</sup>	102.3(6)
O11 – Mn1 – O31 <sup>#</sup>	82.9(1)	N35 – Mn1 – N35 <sup>#</sup>	112.5(7)
O11 – Mn1 – N35 <sup>#</sup>	163.3(4)		

**Table S3.** Selected bond distances (Å) and angles (°) for compound **2**.

<i>d</i> Å			
Cu2-O6	1.894(3)	Cu2-N3	1.919(3)
Cu2-O7	1.898(3)	Cu2-N4	1.908(3)
Mn-O6	2.192(2)	Mn-O13	2.153(3)
Mn-O7	2.191(3)	Mn-O14	2.141(3)
Mn-O23	2.164(3)		
Mn-O5	2.585(3)	Mn-O8	2.624(2)
Cu1-O2	1.905(3)	Cu1-N1	1.942(3)
Cu1-O3	1.916(3)	Cu1-N2	1.931(3)
Cu3-O10	1.908(3)	Cu3-N5	1.941(3)
Cu3-O11	1.904(3)	Cu3-N6	1.939(3)
Angles (°)			
O6-Mn-O7	69.71(9)	O7-Mn-O23	143.7(1)
O6-Mn-O23	145.1(1)	O13-Mn-O14	173.1(1)
O7-Mn-O8	63.78(8)	O8-Mn-O23	81.30(9)
O5-Mn-O23	81.77(9)	O5-Mn-O6	64.16(8)
Cu2-O6-Mn	103.9(1)	Cu2-O7-Mn	103.7(1)

**Table S4.** Selected bond distances (Å) and angles (°) for compound **3**.

<i>d</i> Å			
Cu2-O6	1.894(1)	Cu2-N3	1.921(1)
Cu2-O7	1.897(1)	Cu2-N4	1.911(2)
Mn-O6	2.222(1)	Mn-N8	2.180(2)
Mn-O7	2.179(1)	Mn-N8'	2.269(2)
Mn-N5	2.146(2)		
Mn-O5	2.546(1)	Mn-O9	2.597(1)
Cu1-O2	1.898(1)	Cu1-N1	1.923(2)
Cu1-O3	1.892(1)	Cu1-N2	1.931(1)
Na-O1	2.680(1)	Na-O6	2.910(1)
Na-O2	2.326(1)	Na-O8	2.314(2)
Na-O3	2.344(1)	Na-N5	2.494(2)
Na-O4	2.681(1)		
Angles (°)			
O6-Mn-O7	69.69(4)	O6-Mn-N8	143.98(5)
O7-Mn-N8	138.48(6)	N5-Mn-N8'	171.89(6)
O5-Mn-O6	63.68(4)	O5-Mn-N8	84.81(5)
O7-Mn-O9	64.06(5)	O9-Mn-N8	82.96(5)
Cu2-O6-Mn	102.46(5)	Cu1-O7-Mn	103.96(5)
Mn-N8-Mn'	104.55(6)		

**Table S5.** SHAPE measures for the Mn<sup>II</sup> cations of complexes **1-3** parametrized.  $S(P) = 0$  corresponds to a structure fully coincident in shape with the reference polyhedron P, regardless of size and orientation. The closest polyhedron to the corresponding coordination sphere is highlighted in red.

	(1)	(2)	(3)
$S(\text{vOC-5})$	--	7.00	5.89
$S(\text{TBPY-5})$	--	6.88	6.98
$S(\text{SPY-5})$	--	6.94	5.84
$S(\text{JTBPY-5})$	--	8.86	8.50
$S(\text{OC-6})$	<b>2.03</b>	--	--
$S(\text{TPR-6})$	11.85	--	--
$S(\text{PBPY-7})$	--	<b>1.85</b>	<b>2.84</b>
$S(\text{COC-7})$	--	7.74	5.77
$S(\text{CTPR-7})$	--	6.07	4.48
$S(\text{JPBPY-7})$	--	4.00	5.59

**Ideal ML<sub>5</sub> polyhedra:** vOC-5 (C<sub>4v</sub>) Vacant octahedron; TBPY-5 (D<sub>3h</sub>) Trigonal bipyramid; SPY-5 (C<sub>4v</sub>) Spherical square pyramid; JTBPY-5 (D<sub>3h</sub>) Johnson trigonal bipyramid J12.

**Ideal ML<sub>6</sub> polyhedra:** OC-6 (Oh) octahedron; TPR-6 (D<sub>3h</sub>) trigonal prism

**Ideal ML<sub>7</sub> polyhedra:** PBPY-7 (D<sub>5h</sub>) Pentagonal bipyramid; COC-7 (C<sub>3v</sub>) Capped octahedron; CTPR-7 (C<sub>2v</sub>) Capped trigonal prism; JPBPY-7 (D<sub>5h</sub>) Johnson pentagonal bipyramid J13; JETPY-7 (C<sub>3v</sub>) Johnson elongated triangular pyramid J7.

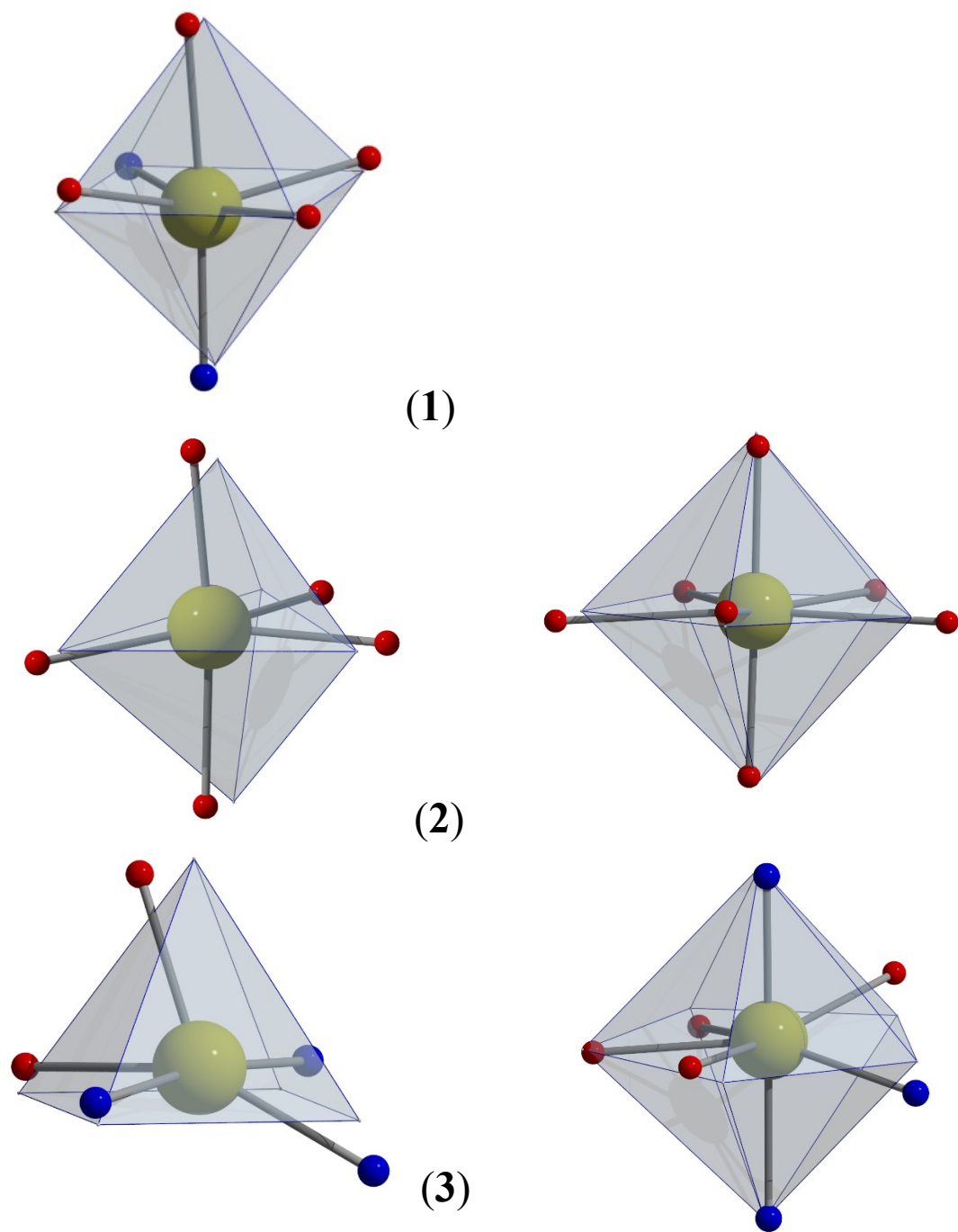


**Figure S2.** Plot of the coordination sphere for complexes **1-3**, referenced to the ideal polyhedron with lower  $S(P)$  value.

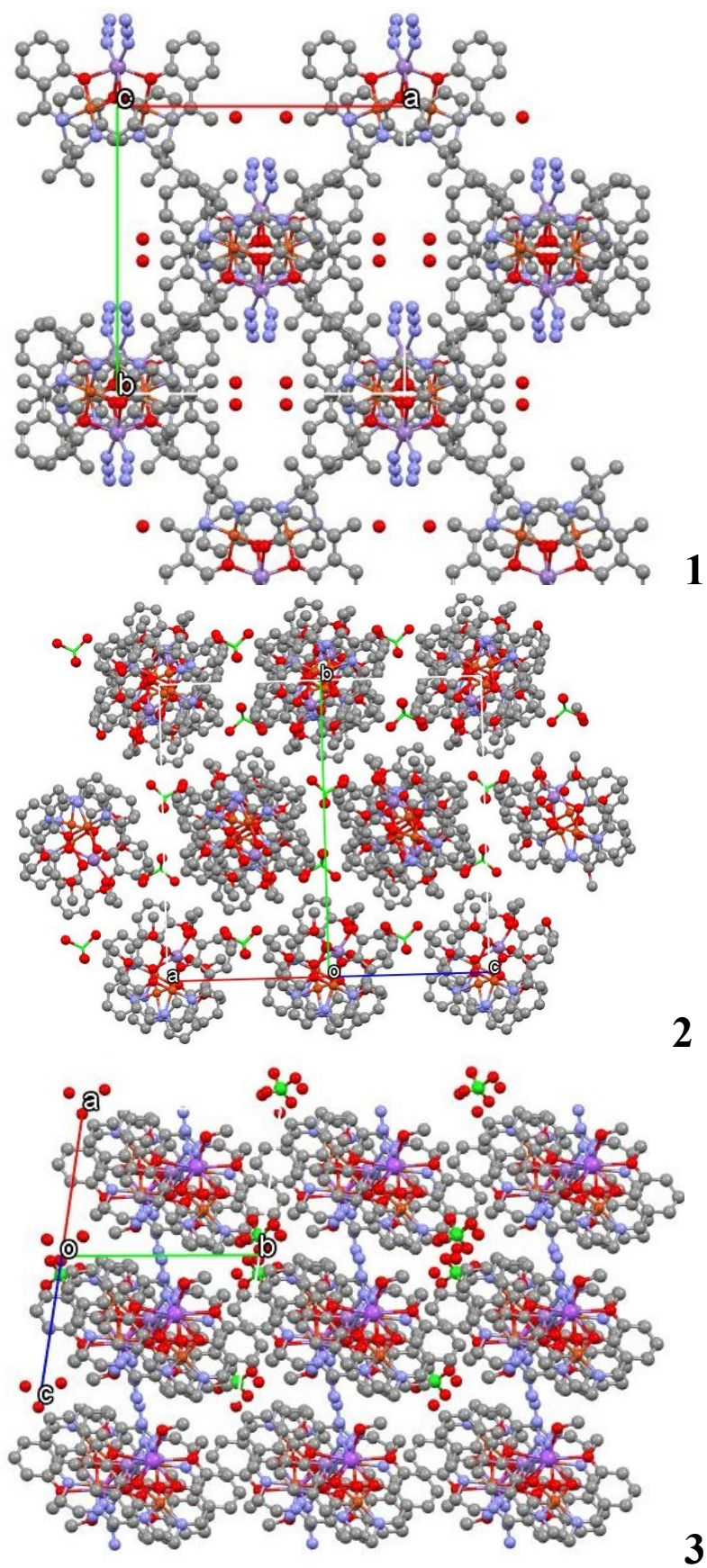


**Figure S3.** Plot of the network arrangement of complexes 1-3 viewed along the pillared clusters.



## 4-Magnetic data.

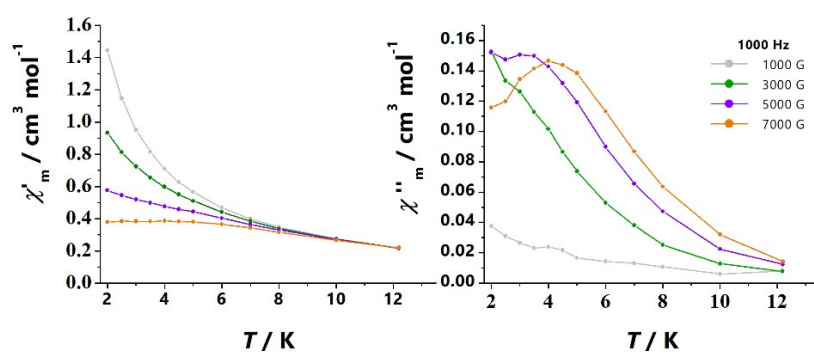


Figure S4.  $\chi_M''$  dependence of the transverse field for complex 1.

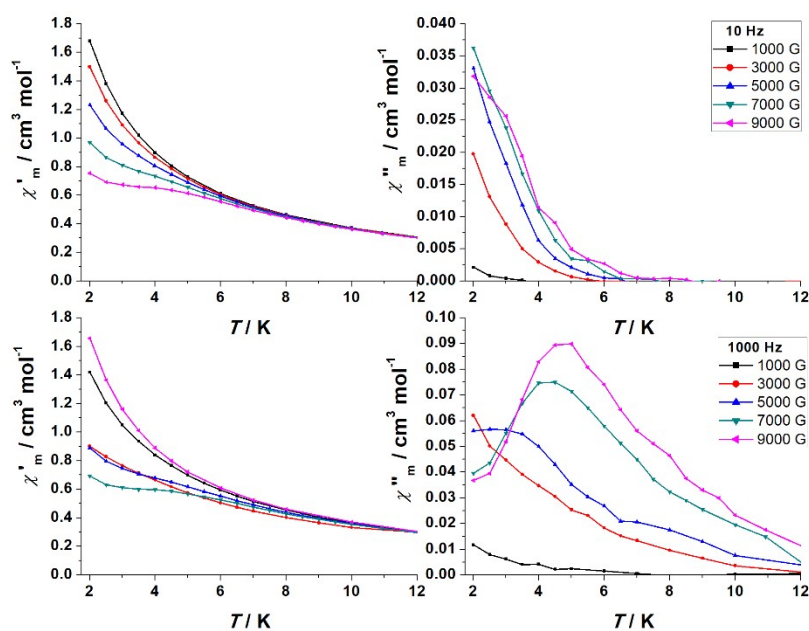


Figure S5.  $\chi_M''$  dependence of the transverse field for complex 2.

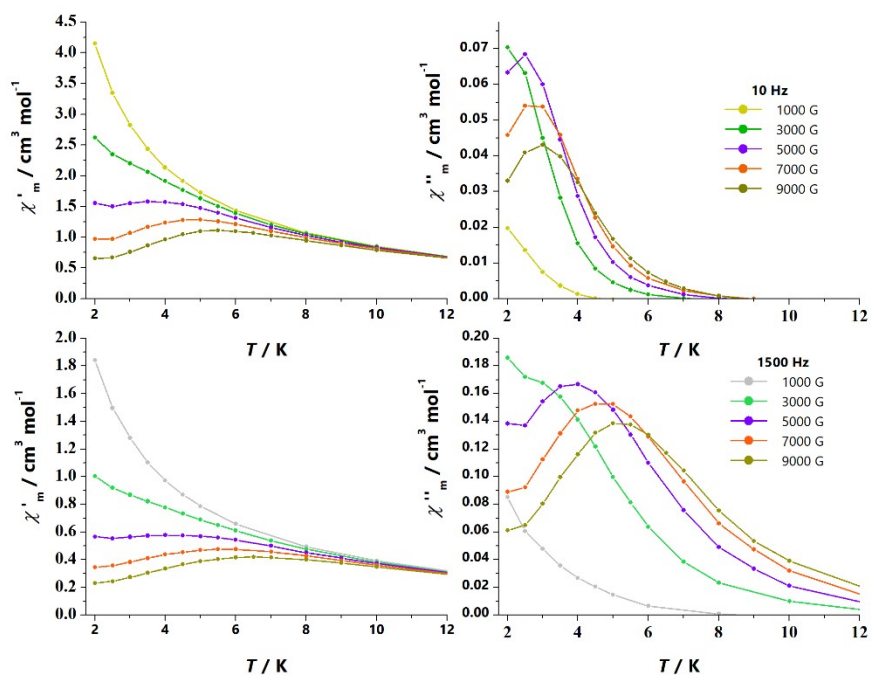


Figure S6.  $\chi_M''$  dependence of the transverse field for complex 3.

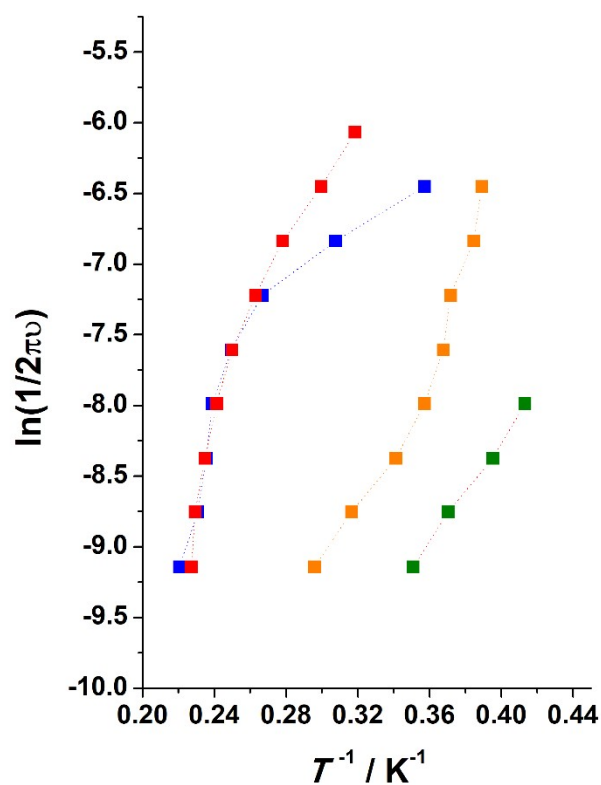
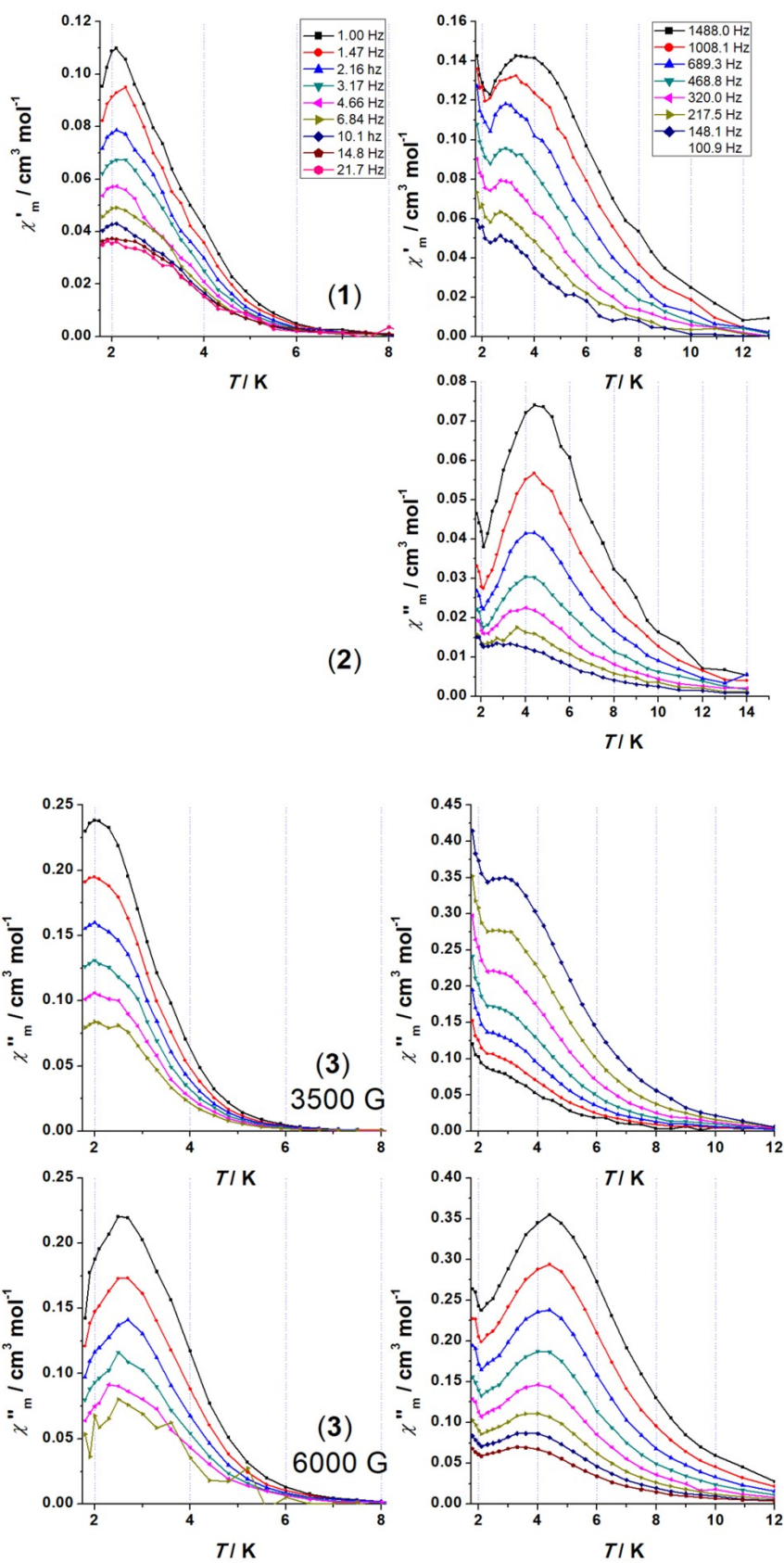
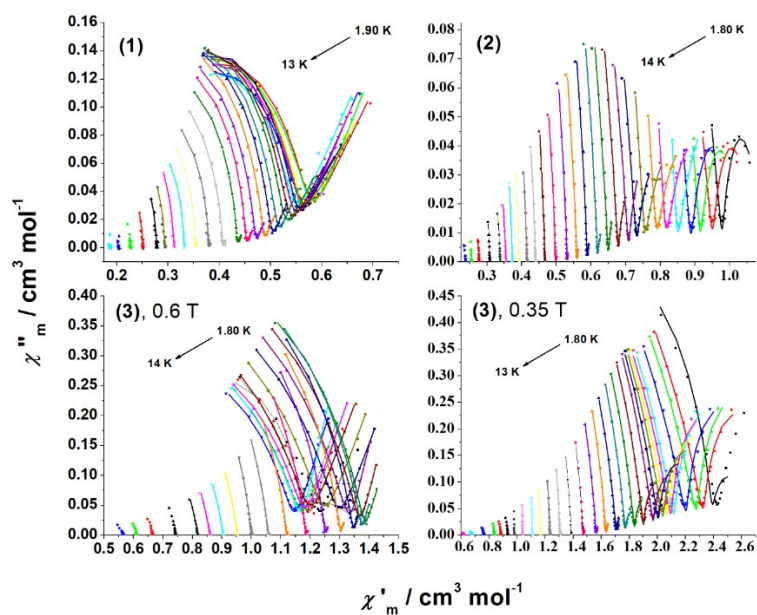


Figure S7. Plot of  $\ln(1/2\pi\nu)$  vs.  $T^{-1}$  from the  $\chi_M''(T)$  data for complexes 1 (orange) 2 (blue) and 3 (3500 G, green; 6000 G, red). The data is limited to the HF region for which the maxima of  $\chi_M''$  can be observed.



**Figure S8.**  $\chi''_m(T)$  for complexes 1, 2 and 3 showing that the position of the maxima is temperature independent for the lower frequencies (left) and temperature dependent for the higher (right) frequencies. For the intermediate range of frequencies maxima are not defined.



**Figure S9.** Cole-Cole plots for complexes **1**, **2** and **3**. Solid lines show the best fit of the experimental data.

**Table S6.** Best fit values for the  $\ln(\tau)$  vs.  $T^{-1}$  plot ( $\frac{1}{\tau} = CT^n + AT + QT$ ) for complexes **1-3**.

	$C$	$n$	$QT$	$A$	$E_a^*$	$\tau_0^*$
<b>(1)</b>	2.011	4.38	9745	--	13.5	$2.9 \cdot 10^{-6}$
<b>(2)</b>	0.001	8.4	--	20714	42.8	$4.9 \cdot 10^{-8}$
<b>(3) - 3500 G</b>	$2.9 \cdot 10^{-4}$	9.1	--	1847	32.5	$1.8 \cdot 10^{-8}$
<b>(3) - 6000 G</b>	0.95	5.23	--	6232	45.2	$6.7 \cdot 10^{-8}$

\*Values extracted from the higher temperature data. Due to the limited number of points these values have a large degree of uncertain.

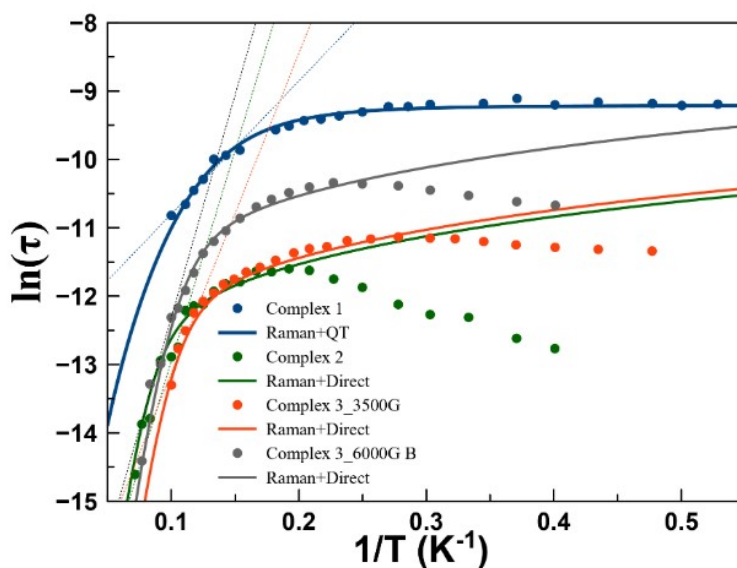


**Figure S10.** Plot of  $\ln(\tau)$  vs.  $T^{-1}$  for complexes **1 – 3**. Solid lines show the best fit of the experimental data. For **2** and **3** the fit was performed for the increasing high temperature data. A after the maximum of the plot the decrease of  $\ln(\tau)$  at lower temperatures. Straigh solid lines (gray), shows the slope of the linear region at higher temperatures.

## References

1. P. Mahapatra, S. Ghosh, S. Giri, V. Rane, R. Kadam, M. G. B. Drew and A. Ghosh, *Inorg. Chem.*, 2017, **56**, 5105.
2. I. Correia, J. C. Pessoa, M. T. Duarte, M. F. M.da Piedade, T. Jackush, T. Kiss, M. M. C. A. Castro, C. F. G. C. Geraldes and F. Avecilla, *Eur. J. Inorg. Chem.*, 2005 , 732.